Annals of Nuclear Medicine Vol. 8, No. 4, 245–251, 1994

Assessment of dopamine metabolism in brain of patients with dementia by means of ^{18}F-fluorodopa and PET

Masatoshi ITOH,[1] Kenichi MEGURO,[2] Takehiko FUJIWARA,[1] Jun HATAZAWA,[3] Ren IWATA,[4] Kiichi ISHIWATA,[5] Toshihiro TAKAHASHI,[6] Tatsuo IDO[4] and Hidetada SASAKI[2]

[1]*Division of Nuclear Medicine,* [4]*Division of Radiochemistry, Cyclotron RI Center, Tohoku University*
[2]*Department of Geriatrics, Tohoku University School of Medicine*
[3]*Department of Radiology, Institute of Brain and Blood Vessels, Akita*
[5]*Positron Medical Center, Tokyo Metropolitan Institute for Aging*
[6]*Radioisotope Center, Niigata University*

By means of positron emission tomography (PET) and ^{18}F-fluorodopa (FDOPA), a study was initiated to analyze the cerebral dopamine (DA) metabolism of 32 subjects including those with AD/SDAT and vascular dementia (VD, multi-infarct type). A semiautomated irregular ROI drawing routine to identify the striatum was developed that interactively defined the PET threshold pixels referring to the count histograms and location of the corresponding pixels. A comparative study by five examiners showed significant improvement in the area size definition and count linearity particularly for low contrast objects. The graphical plot was employed to calculate the FDOPA influx rate (Ki) for the ROI data with cerebellar radioactivity as an input function. The striatal Ki value was found to be relatively stable and did not show signs of a significant age-related change. The vascular patients had smaller Ki to the striatum than the aged control. Although the mean Ki of AD/SDAT was almost compatible with that of age-matched normals, their Ki was more scattered with higher and lower Ki cases. The multiple regression analysis revealed that the Ki could be predicted by age and the mini-mental state (MMS) performance ($r^2 = 0.590$, $p < 0.01$ for AD/SDAT, $r^2 = 0.401$, and $p < 0.05$ for VD). MMS was found to be a more dominant factor than age. We conclude that dopamine metabolism became disturbed as dementia became progressively severe.

Key words: Neurotransmission, PET, dementia, DOPA metabolism

INTRODUCTION

NIGRO-STRIATAL DOPAMINERGIC INNERVATION plays a fundamental role in regulating extrapyramidal motor systems. A part of the system is linked to the neocortex and limbic brain.[1] The nucleus accumbens or the ventral striatum connects to the amygdala, ventral pallidum, thalamus, the limbic and premotor cortex and functions as an interface between the limbic and the motor systems. It is thought to be related to the temporal control of behavior, reward-related learning and memory function.[2] It is reasonable to assume, therefore, that the dopaminergic system plays numerous roles in the manifestation of symptoms associated with dementia. This hypothesis is supported by the fact that a proportion of patients with dementia of the Alzheimer type, especially those who suffer a more rapid intellectual decline[3,4] have extrapyramidal signs e.g. rigidity, tremor, and bradykinesia. Positron emission tomography (PET) permits assessment of cerebral metabolism *in vivo* at various stage of dementia. Recently, measurements of blood flow, glucose consumption, and other physiological parameters have been increasingly employed to evaluate cerebral metabolism and the dopamine metabolism in the cerebrum can be assessed with ^{18}F-fluorodopa as a labeled agent mostly in movement disorder patients.[5,6] The purpose of the present study was to elucidate disturbances in the dopaminergic function in the brains of demented patients.

Received February 4, 1994, revision accepted June 30, 1994.
For reprint contact: Masatoshi Itoh, M.D., Division of Nuclear Medicine, Cyclotron Radioisotope Center, Tohoku University, Aoba, Aramaki, Aoba-ku, Sendai 980, JAPAN.

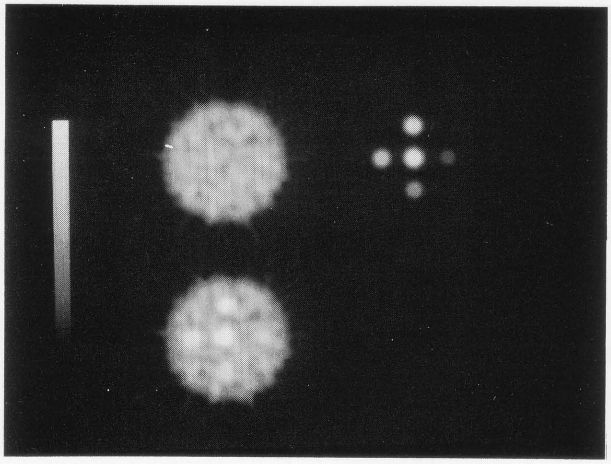

Fig. 1 Phantom images for the threshold-ROI performance test. A cylindrical phantom of 15 cm inner diameter filled with $^{18}F^-$ solution (top left). Five rods of 2.0 cm in diameter were synthesized from the point spread function of our PET system (6.0 mm FWHM, top right). The peak count of the rods were adjusted so that the peak count of each rod have 20, 40, 60, 80 and 100% higher count than the phantom radioactivity. Addition of the rods with the phantom formed a test phantom for ROI performance.

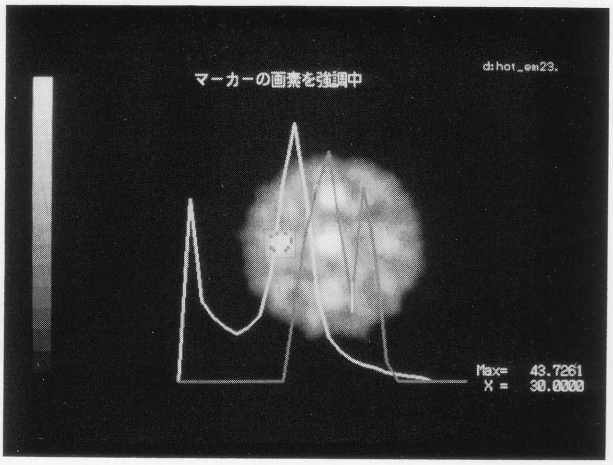

Fig. 2 Threshold ROI. The program generates two count histograms, one (white line) for the whole image and the other (gray line) within the target area (the left rod). The operators choose the threshold count referring the histograms and anatomical locations of the chosen pixels. The abscissa and the ordinate express PET count and pixel number, respectively.

METHODS

Phantom experiment: To validate our ROI drawing routine described below, a phantom experiment was carried out with a cylindrical phantom (15 cm inner diameter and 25 cm in length) filled with 1.11 mCi of F^- solution. The phantom was measured three times for 5, 10, and 30 minutes to have the count variation similar to the usual FDOPA brain images. Actually a summed image generated from two planes, i.e., the number 3 and 5 plane of 5 minute scan was chosen as a test phantom that had 0.0212 ± 0.0397 cps/pixel (coefficient variation was 18.7%) as the average. Five rods of the same 20 mm diameter size were generated from the point spread function of our system, i.e., 6.0 mm at FWHM. Their peak count was varied from 20 to 100% of the average count of the test phantom with 20% increases. Finally the rods were summed on the test phantom as shown in Figure 1.

ROI program and its performance test

Two irregular ROI draw routines were applied on the phantom by five examiners who were informed only of the location of the rods. A ROI program (irregular ROI) prompted setting points sequentially at the object boundary and the other, which we named the "threshold ROI," prompted to choose the threshold PET value for the object. The chosen PET threshold was marked both on the PET image and on the pixel count histograms of the whole image and of the target area (around the object). The operators can select an appropriate threshold PET value by interactively moving a cursor on the histogram (Fig. 2). Finally the pixels which fell between the upper and lower thresholds were picked up and subjected to the statistical calculation.

PET measurement: Fluorine-18 was produced at the Cyclotron RI Center, Tohoku University and 6-^{18}F-L-FDOPA was synthesized according to the method described by Adam et al.[7] Following an intravenous bolus injection of FDOPA (2.5–8.3 mCi, specific activity between 167–686 mCi/μmol) into the subjects, positron tomography was carried out parallel to the orbito-meatal (OM) line by using PT931 (CTI Inc, USA) with 7 mm axial and transaxial resolution.[8] Emission scans were performed every 5 minutes for 60 min after the injection. The emission data were corrected for tissue attenuation with transmission data collected by means of a ^{68}Ge/Ga cylinder source.

PET data analysis: The tissue FDOPA concentration was measured defining ROIs on three image planes that included the striatum. Sequential PET images, taken over a period of 40–60 minutes, were added to improve the signal/noise ratio. The striatum was defined on this summated image by means of the threshold ROI program that calculated the area size and average PET value for each dynamic frame. The other brain regions such as the frontal, temporal, occipital cortices, and the cerebellum were defined by means of the ellipsoid ROI drawing routine. The rate of influx (Ki) of FDOPA into the selected regions was then calculated by the graphical analysis described by Patlak et al.[9,10] with the concentration of the cerebellum radioactivity as the input function. A linear fitting was carried out with data between 25 and 60 min post FDOPA injection. A typical case is shown in Figure 3.

Subjects: Studies were performed on thirty-two

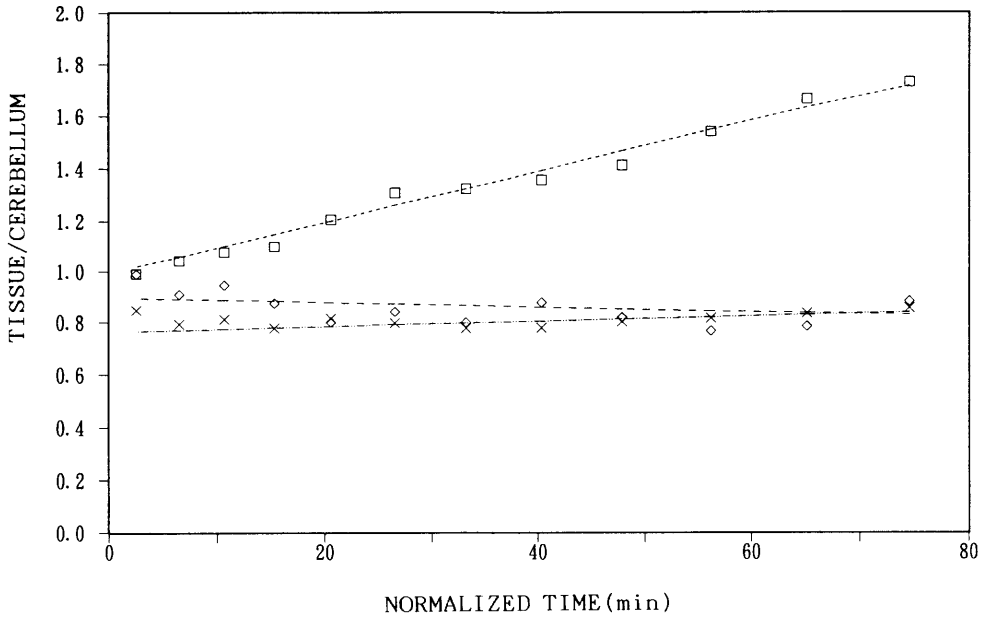

Fig. 3 Graph plots of a dementia case. PET count ratios as the tissue/cerebellum were plotted against the normalized time that was the integrated cerebellum count from 0 time up to PET scan time over cerebellum instantaneous count. The linear regressions were obtained using the final seven points (□ striatum, × frontal cortex, ◇ occipital cortex).

Table 1 Comparison of ROI taking of five hot spots (rod) by five operators between using irregular ROI draw routine and using the threshold-ROI routine. The operators were asked to define regions with no information of rod size and their relative count.

	ROI value (count)					ROI area (pixels)					
rod#	1	2	3	4	5	1	2	3	4	5	mean
Irregular-ROI											
color mean	169	161	155	131[$]	128[$]	58	97	60	76	35	65
s.d.	8	6	6	16	5	11	47	11	36	15	35
b/w mean	176	162	144	130[$]	127[$]	74	63	79	84	41	68*
s.d.	6	6	23	20	6	45	12	55	52	15	43
Threshold-ROI											
mean	184	167	158	141	131	48	53	49	57	32	48*
s.d.	11	4	3	3	6	9	16	8	13	19	16
True count (%)[1)]	200	180	160	140	120	Actual size = 50					

Irregular ROI were defined on either color or white on black CRT display. * $p < 0.05$ by multiple comparison with Bonferroni's correction. [$] no difference between rod4 and rod5. [1)] % relative to the background.

subjects over 50 years old including 11 normal subjects (6 males and 5 females; average age: 63.3 ± 9.2),12 patients with Alzheimer's disease and senile dementia (AD/SDAT) (5 males and 7 females; average age: 67.0 ± 11.3) and 9 patients with vascular dementia (5 males and 4 females; average age: 74.1 ± 6.9). The diagnosis of dementia was based on DSM-III-R.[11] The dementia subtypes were judged mainly on the clinical profiles of symptoms, referenced to the Ischemic Score[12] and CT/MRI findings. The severity of the dementia was evaluated with the mini-mental state battery (MMS). CT and MRI were performed in all the subjects. The existence of any ischemic lesion other than lacuna excluded the subject from the study. The striatum was morphologically normal in all AD/SDAT subjects. One patient with vascular dementia had a small lacuna in one side of the striatum and other two subjects had lacunae in the white matter. Neurological examination revealed no focal abnormality in AD/SDAT cases except for one patient who showed mild muscular weakness in the left unilateral limbs. Three vascular patients had unilateral hemiplegia and two cases had muscular rigidity. Statistical analysis was done by means of the correlation analysis, one-way or two-way ANOVA and multiple comparison with Bonferroni's correction.[13]

Table 2 Regional FDOPA Ki in dementia patients calculated by graphical analysis

	Normals	AD/SDAT	Vascular
N	11	12	9
Striatum	0.0116* ± 0.0017	0.0110 ± 0.0031	0.0081* ± 0.0026
Frontal cortex	0.0028# ± 0.0013	0.0028# ± 0.0013	0.0015 ± 0.0007
Temporal cortex	0.0022 ± 0.0013	0.0013 ± 0.0015	0.0018 ± 0.0016
Occipital cortex	0.0008# ± 0.0014	−0.0004# ± 0.0027	0.0002 ± 0.0015

# $p < 0.01$ within groups, * $p < 0.05$
by multiple comparison with Bonferroni's correction

The protocol was approved by the Committee for Clinical Application of Radiopharmaceuticals at Tohoku University. Written and informed consent was obtained from a member of the family of each patient.

RESULTS

Phantom experiment

The average ROI values defined by five examiners at five different hot spots are summarized in Table 1 and Figure 3. For each hot spot ROIs were defined by means of the irregular ROI drawing routine or the threshold-ROI routine on a gray-scale display. The effect of color display was evaluated for irregular ROI draw procedures performed either on the gray scale (W/B) display or rainbow color display. Although full recovery of each peak count was never achieved by means of any ROI program, the mean counts obtained by different ROI methods almost linearly correlated with the real values. The ROI count depended significantly on the ROI procedure ($p < 0.05$ by ANOVA). ROI counts by the threshold-ROI were always ($p < 0.05$) higher than by the irregular ROI drawing method. The rods that had a +20 or +40% higher count than the background were differentiated from each other by the threshold-ROI method only ($p < 0.05$ by multiple comparison) but not by the irregular ROI drawing method. The ROI area depended on the hot spot count ($p < 0.05$, by ANOVA). The area was much less for the +20% rod than others in any ROI procedure. The true area (50 pixels) was most accurately measured by the threshold-ROI method that determined the average area to be 47.6 ± 16.0 pixels. The irregular ROIs overestimated the area (65.0 ± 34.7 pixels for the color image and 68.2 ± 42.9 pixels for the B/W image). The color display somewhat increased reproducibility as seen in the smaller variance in ROI count and area than those defined on W/B display, however the difference did not reach a significant level.

Brain FDOPA influx rate

The Ki of FDOPA influx into the striatum and other cortical regions (average for the two sides) in normal subjects and two types of dementia are summarized in Table 2. Two way ANOVA revealed that the Ki for the striatum and all cortical regions differed significantly (F-value = 155.3, $p < 0.01$). The Ki to the occipital cortex was negligible (0.00006 ± 0.00207 min^{-1}) and smaller than the frontal and temporal cortex ($p < 0.01$ by multiple comparison). The striatal Ki of the normal group was 0.0116 ± 0.0017 min^{-1} and showed no age-related decline ($Ki = -0.00003 \cdot Age + 0.01333$, $r = -0.152$, Fig. 4). The striatal Ki differed significantly among study groups (F-value = 5.03, $p < 0.01$, by ANOVA, Table 2). The vascular dementia group had a lower striatal Ki (0.0081 ± 0.0026 min^{-1}) than normals (0.0110 ± 0.0031 min^{-1}, $p < 0.05$, by multiple comparison). The multiple regression analysis revealed that the Ki could be predicted by age and dementia severity as evaluated with the mini-mental state as $Ki = -0.000046 \cdot Age + 0.000382 \cdot MMS + 0.008076$ ($r^2 = 0.590$, $p < 0.01$) for AD/SDAT and $Ki = -0.000088 \cdot Age + 0.000226 \cdot MMS + 0.010483$ ($r^2 = 0.401$, $p < 0.05$) for vascular dementia. The MMS term in AD/SDAT was most significant with its t-value as 3.168 ($p < 0.01$). The correlation analysis supported the dependence of Ki on MMS rather than on age (Figs. 5 and 6). PET images of typical cases are shown in Figure 7.

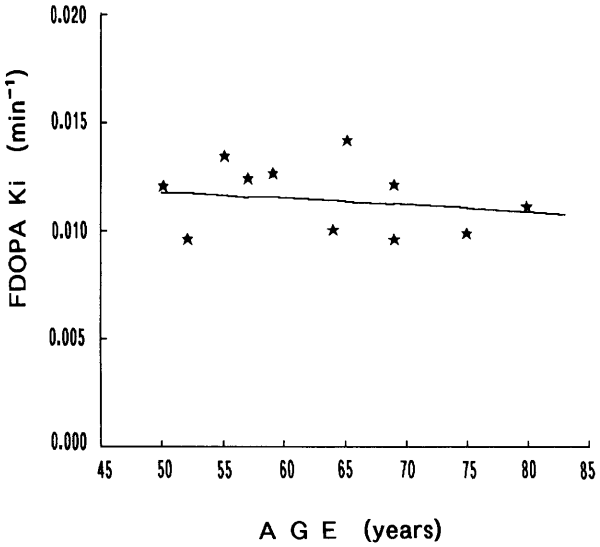

Fig. 4 Age effect on FDOPA influx rate (Ki) into the striatum of normal subjects. The correlation was not significant.

DISCUSSION

Diagnosis of the dementia subtype of our patients was based on clinical findings and brain anatomical informa-

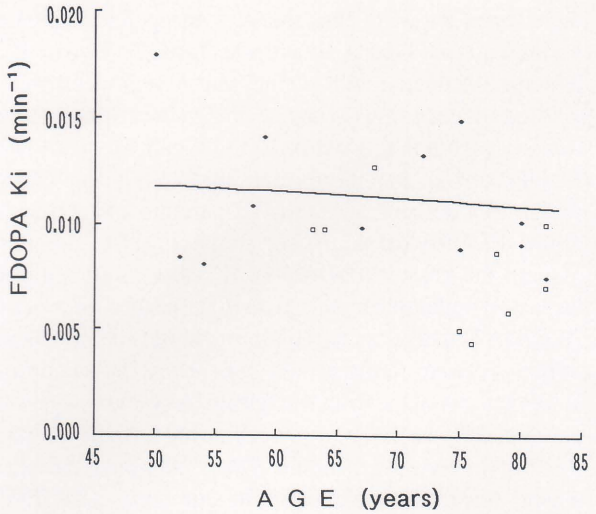

Fig. 5 Age effect on the FDOPA influx rate into the striatum of dementia patients. The regression line for normal controls are also shown. (◆) AD/SDAT, (□) vascular dementia.

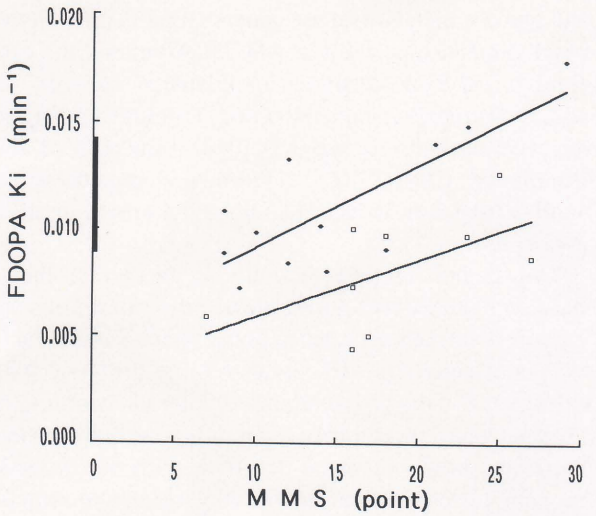

Fig. 6 The correlation of the striatal FDOPA influx rate and dementia severity as assessed with the mini-mental state battery (MMS). Data is shown for the AD/SDAT (◆) and vascular dementia (□). The range of normals is shown along *Y*-axis.

tion on CT and MRI images. All the subjects were discussed at the Dementia Clinical Conference, which was attended by a number of doctors including neurologists, psychologists, radiologists, gerontologist and neuropathologists. This procedure would have helped to improve diagnostic objectivity. The distribution of the patients' age was almost identical for the controls and the patients with AD/SDAT, but, the patients with vascular dementia included older subjects compared to the other groups although the difference between groups in age distribution was not significant by one way ANOVA. Because there was no correlation between the rate of FDOPA uptake and age in any three subject groups, the age effect hardly explains the reduced FDOPA metabolism in the patients with vascular dementia.

The measurement of cerebral metabolism *in vivo* is often conducted by compartment analysis, which requires frequent sampling of the arterial blood during tracer circulation. The concept of compartment assumes that the radioactivity in each compartment is derived from a simple chemical component. It has been proved, however, that FDOPA is readily metabolized into several metabolites such as fluorodopamine, fluoroDOPAC, fluoromethyl DOPA (MeFDOPA), etc.[14,15] It is not valid, therefore, to adopt simple compartments in the brain in the FDOPA model. Poor compliance by demented patients made it difficult to keep them in the same study position for a sufficient length of time. Because only minimum PET measurement could be recorded, the quantification model had to be simple. Patlak, et al. proposed graphical analysis[9,10] as a method to estimate tracer influx to the irreversible compartment. Hoshi, et al.[16] reported a fairly good correlation between values obtained by the graphical analysis and by compartment analysis in normal subjects. They also shown that FDOPA influx rates calcu-

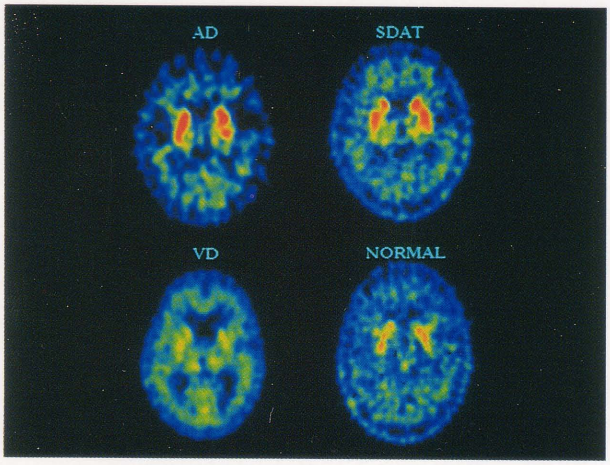

Fig. 7 PET images of representative cases. Top left: 50 y.o. female, AD, MMS 28. Ki 0.0172 min^{-1}. Top right: 80 y.o. male, SDAT, MMS 18, Ki 0.00907 min^{-1}. Bottom left: 76 y.o. female, VD, MMS 16, Ki 0.00434 min^{-1}. Bottom right: 57 y.o. female, normal subject, Ki 0.01340 min^{-1}. Images are summation between 40 to 60 min after injection. The display was adjusted such that cortices had the same level.

lated with cerebellum radioactivity were better estimates of FDOPA decarboxylase activity than those calculated with metabolites corrected plasma radioactivity. Although FDOPA Ki reflects over-all dopa metabolism, it may be affected by blood-brain barrier permeability and cerebral blood flow as well, which might be altered in pathological conditions. We assumed that the transfer rate of FDOPA from capillary to brain tissue was identical between in both the striatum and the cerebellum. Thus, in the case of reduced FDOPA availability in the striatum relative to the cerebellum, striatal Ki may be underestimated due to overestimation of the input function. Cerebral blood flow

and glucose metabolism are generally maintained in the basal ganglia, especially in AD.[17–19] Although, the cerebral blood flow decreases in dementia patients, its striatum/cerebellum ratio remained very close among age matched controls (0.94), AD (0.90), and VD of the Binswanger type (0.98).[20] Blood flow change therefore hardly explains the reduced FDOPA uptake in the striatum in our case.

The method of data sampling is another problem. Because of limited resolution the boundary of the objects is blurred and their apparent radioisotope concentration is always affected by the partial volume problem. The examiners usually define regions of interest according to a certain visual threshold of color or gray scale intensity. We tested how examiners define the regions, without knowing the object size and intensity, using five synthesized hot rods in the background that had count a variation similar to the usual FDOPA brain images. As a result the ROI area was overestimated by 30 to 36% with an irregular ROI drawing procedure. The coefficient of variation for the ROI area could be as great as 63%. This means that ROI takings are highly dependent on the examiners. The reason for this is insufficient informations. We introduced a threshold ROI program that incorporated PET count histograms. The chosen threshold for the boundary was marked on a PET image and on histograms interactively. We found that the count histogram of all the image pixels was so broad that the histogram for the target area was required. A comparative trial by five examiners showed significant improvement in area definition and count linearity; the measured area size was very close to the actual size (only 5% underestimation in average and the coefficient of variation reduced from 13.1% (irregular ROI on W/B images) to 6.0% ($p < 0.05\%$ by multiple comparison). The threshold ROI method therefore seemed to be superior to the visual ROI drawing routine, particularly for low contrast objects. Naturally, it was not able to solve the problem of partial volume phenomenon and exact peak counts were never estimated by this method.

Postmortem studies revealed that there are age-related reductions in the concentration of DA in the caudate nucleus in the group of patients older than 65.[21] PET observation of a normal aged population also found a gradual decline in FDOPA uptake with age.[22] However, a recent study cast doubt on this age-related decline.[23] Our data support the latter. We reported the stability of blood flow and oxygen metabolism in neurologically normal populations up to 80 years of age.[24] Little change in FDOPA uptake in normal subjects strongly supports the concept of preserved homeostasis in brain metabolism in the normal population.

Tyrrell, et al.[25] reported no significant changes in FDOPA uptake into the caudate and putamen in Alzheimer type dementia patients with extrapyramidal signs. However, they found a greater variance in Ki values for FDOPA in the patients' group than in normal subjects. Our data agree with theirs showing that the AD group had a greater variance in the FDOPA uptake rate (Table 2). Two of their patients had putaminal Ki values that were lower than the 99% confidence limit of the normal values. It was therefore suggested that some AD/SDAT patients had lower FDOPA uptake than the normal subjects. It is noteworthy that mildly demented AD/SDAT patients had relatively higher FDOPA uptake in our study (Fig. 6). This may explain the greater variance in Ki values and suggests increased dopamine metabolism in the early course of the AD/SDAT. There are some reports about reciprocal activities between cortical and subcortical DA neurons. Underactivity of the frontal cortical DA system may result paradoxically in overactivity of the subcortical DA projection (see review by Robbins TW).[26] Although the exact reason for DA hyperactivity in our early AD/SDAT patients is not known, it may reflect a disturbed neuronal function including the striatal DA system. The DA and HVA of human postmortem specimens were reported to be significantly reduced in AD/SDAT patients (for a review, see Gottfries, C.G.).[27] DA metabolism must therefore be disturbed in AD/SDAT, especially in the final stage. In the case of vascular dementia, the concentration of DA also decreased in the caudate nucleus compared with the brains of age-matched controls.[28] This may be related to the vulnerability of the striatum to ischemia.

Neurological examination revealed mild muscular weakness in the left unilateral limb in one AD/SDAT patient. The rest of the subjects showed no clinical neurological sign including parkinsonism. Two patients with vascular dementia showed unilateral or bilateral muscular rigidity and tremor. The FDOPA influx rate for these patients did not differ from the average for the vascular dementia group. Thus, their symptoms were hardly explained by reduced dopamine metabolism only. Our value for Parkinson's disease patients was less than half of that for the normal age-matched control.[29] The average striatal Ki value in patients with vascular dementia was 77% of normal controls in the present study. Thus, the level of reduced dopamine uptake in our dementia patients was not severe enough to lead to overt Parkinson's disease symptoms.

CONCLUSION

Our results demonstrated that central dopamine metabolism is gradually impaired in the progression of the dementia process in both AD/SDAT and vascular dementia. The degree of reduction was rather small compared to the reported values for Parkinson's disease that also accompanies mental deterioration only in the advanced stage. The underlining mechanism for the reduction of dopamine metabolism might therefore be different when compared with dementia as observed in Parkinson's disease.

ACKNOWLEDGMENTS

The authors wish to thank the members of CYRIC of Tohoku University for supporting the study. A part of this work was supported by Grants-in-Aid from Ministry of Health and Ministry of Education. Part of the present study was reported at the 6th Medical Application of Cyclotrons, Turku, 1992, and at the 16th International Symposium on Cerebral Blood Flow and Metabolism, Sendai, 1993.

REFERENCES

1. Scatton B, Zivkovic B. Neuroleptics and the limbic system. *In* Psychopharmacology of the limbic system. Trimble MR & Zarifian E (eds.), Oxford, Oxford University Press, pp. 174–197, 1984.
2. Salamone JD. Behavioral pharmacology of dopamine system: a new synthesis. *In* The mesolimbic dopamine system: from motivation to action. Willner P, Scheel Krueger J (eds.), Chichester, John Wiley & Sons, pp. 599–614, 1991.
3. Mayeux R, Stem Y, Spanton S. Heterogeneity in dementia of the Alzheimer type: evidence of subgroups. *Neurology* 35: 453–461, 1985.
4. Chui HC, Teng EL, Henderson V, Moy AC. Clinical subtypes of dementia of the Alzheimer type. *Neurology* 35: 1544–1550, 1985.
5. Nahmias C, Garnett ES, Firnau G, Lang A. Striatal dopamine distribution in Parkinsonian patients during life. *J Neurolog Sci* 69: 223–320, 1985.
6. Leenders KL, Palmer AJ, Quinn N, Clark JC, Firnau G, Garnett ES, et al. Brain dopamine metabolism in patients with Parkinson's disease measured with positron emission tomography. *J Neurol Neurosurg Psychiat* 49: 853–860, 1986.
7. Adam MJ, Abeysekera B, Ruth TJ, Grierson JR, Pate BD. Synthesis of 6-(F-18)L-fluoro-dopa using F-18 labeled acetyl hypofluorite. *J Nucl Med* 26: P125, 1985.
8. Watanuki S, Ishii K, Orihara H, Fukuda H, Matsuzawa T. Status of multi-ring high-resolution positron emission tomography system PT931. CYRIC Annual Report 1986: 250–244, 1986.
9. Patlak CS, Blasberg RG. Graphical evaluation of blood-to-brain transfer constants from multiple-time uptake data. Generalizations. *J Cereb Blood Flow Metabol* 5: 584–590, 1985.
10. Patlak CS, Blasberg RG, Fenstermacher JD. Graphical evaluation of blood-to-brain transfer constants from multiple-time uptake data. *J Cereb Blood Flow Metabol* 3: 1–7, 1983.
11. American Psychiatric Association. *Diagnostic and Statistical Manual of Mental Disorders*. DSM-III-R. Washington DC, Amer Psychiat Ass, pp. 103-122, 1987.
12. Hachinski VC, Iliff LD, Zilka E, DuBoulay GH, McAllister VL, Marshall J, et al. Cerebral blood flow in dementia. *Arch Neurol* 32: 632–637, 1975.
13. Tanaka Y, Tarumizu T. *Handbook on Statistics on PC*, III. Tokyo, Kyoritsu Shuppan Inc., pp. 1–15, 1986.
14. Firnau G, Sood S, Chirakal R, Nahmias C, Garnett ES. Metabolites of 6-[^{18}F]fluoro-L-dopa in the human blood. *J Nucl Med* 29: 363–369, 1988.
15. Melega WP, Hoffman JM, Luxen A, Nissenson CHK, Phelps ME, Barrio JR. The effects of carbidopa on the metabolism of 6-[F-18]fluoro-L-dopa in rats, monkeys and humans. *Life Sci* 47: 149–157, 1990.
16. Hoshi H, Kuwabara H, Leger G, Cumming P, Guttman M, Gjedde A. 6-[^{18}F]fluoro-L-DOPA metabolism in living human brain: A comparison of six analytical methods. *J Cereb Blood Flow Metab* 13: 57–69, 1993.
17. Rapoport SI. Positron emission tomography in Alzheimer's disease in relation to disease pathogenesis: a critical review. *Cerebrovasc Brain Metab Rev* 3: 297–335, 1991.
18. Meyer JS, Terayama Y, Takashima S. Cerebral circulation in the elderly. *Cerebrovasc Brain Metab Rev* 5: 122–146, 1993.
19. Heiss WD, Szelies B, Kessler J, Herholz K. Abnormalities of energy metabolism in Alzheimer's disease studied with PET. *Ann NY Acad Sci* 640: 65–71, 1991.
20. Kuwabara Y, Ichiya Y, Otsuka M, Masuda K, Ichimiya A, Fujishima M. Cerebrovascular responsiveness to hypercapnia in Alzheimer's dementia and vascular dementia of the binswanger type. *Stroke* 23: 594–598, 1992.
21. Carlsson A, Winblad B. Influence of age and time interval between death and autopsy on dopamine and 3-methoxytyramine levels in human basal ganglia. *J Neural Transm* 38: 271–276, 1976.
22. Leenders KL, Salmon EP, Turton D, Tyrrell P, Perani D, Brooks DJ, et al. The nigro-striatal dopaminergic system assessed *in vivo* by positron emission tomography in healthy volunteer subjects and patients with Parkinson's disease. *Arch Neurol* 47: 1290–1298, 1990.
23. Takikawa S, Dahwan V, Chaly T, Robeson W, Spetsieris P, Eidelberg D. Does striatal FDOPA uptake decrease with age? *J Cereb Blood Flow Metab* 13: S410, 1993.
24. Itoh M, Hatazawa J, Miyazawa H, Matsui H, Meguro K, Yanai K, et al. Stability of cerebral blood flow and oxygen metabolism during normal aging. *Gerontology* 36: 43–48, 1990.
25. Tyrrell PJ, Sawle GV, Ibanez V, Bloomfield PM, Leenders KL, Frackowiak RSJ, et al. Clinical and positron emission tomographic studies in the 'extrapyramidal syndrome' of dementia of the Alzheimer type. *Arch Neurol* 47: 1318–1323, 1990.
26. Robins TW. Cognitive deficits in schizophrenia and Parkinson's disease: Neural basis and the role of dopamine. *In* the mesolimbic dopamine system: From motivation to action, Willner P, Sheel-Krueger (eds.), Chichester, Jon Wiley & Sons, pp. 497–528, 1991.
27. Gottfries CG. Neurochemical aspects on aging and diseases with cognitive impairment. *J Neurosci Res* 27: 541–547, 1990.
28. Wallin A, Alafuzoff I, Carlsson A, Eckernaes SA, Gottfries CG, Karlsson I, et al. Neurotransmitter deficits in a nonmulti-infarct category of vascular dementia. *Acta Neurol Scand* 79: 397–406, 1989.
29. Nagasawa H, Saito H, Kogure K, Hatazawa J, Itoh M, Fujiwara T, et al. 6-[^{18}F]fluorodopa metabolism in patients with hemiparkinsonism studied by positron emission tomography. *J Neurolog Sci* 115: 136–143, 1993.